LASER INTERFEROMETER GRAVITATIONAL WAVE OBSERVATORY
- LIGO -
CALIFORNIA INSTITUTE OF TECHNOLOGY
MASSACHUSETTS INSTITUTE OF TECHNOLOGY

Technical Note **LIGO-T2300207–v2** 2023/09/22

Feed Forward Frequency Stabilization of 2 Micron Lasers Using Optical Delay Homodyne Interferometry

Hannah Rose

California Institute of Technology
LIGO Project, MS 18-34
Pasadena, CA 91125
Phone (626) 395-2129
Fax (626) 304-9834
E-mail: info@ligo.caltech.edu

Massachusetts Institute of Technology
LIGO Project, Room NW22-295
Cambridge, MA 02139
Phone (617) 253-4824
Fax (617) 253-7014
E-mail: info@ligo.mit.edu

LIGO Hanford Observatory
Route 10, Mile Marker 2
Richland, WA 99352
Phone (509) 372-8106
Fax (509) 372-8137
E-mail: info@ligo.caltech.edu

LIGO Livingston Observatory
19100 LIGO Lane
Livingston, LA 70754
Phone (225) 686-3100
Fax (225) 686-7189
E-mail: info@ligo.caltech.edu

http://www.ligo.caltech.edu/

Contents

1 Abstract

The proposed post-O5 LIGO Voyager upgrade as well as some proposed third-generation gravitational wave observatories center on a cryogenic silicon optics system for reduced thermal noise. This requires a shift of the laser wavelength further to the infrared using the comparatively noisy 2-micron technology to compensate for the high absorption of the current 1064nm laser in crystalline silicon. To meet the tight frequency noise requirements for desired sensitivities of these interferometers, we demonstrate a feed-forward frequency noise reduction system at 2050nm in fiber. Additionally, we characterize the sources of noise limiting the degree of noise reduction and the sensitivity of the interferometric measurement of the reduced frequency noise, allowing for the targeting of future improvements to the system.

2 Introduction

From LIGO's observation of gravitational waves to timing experiments, laser systems are critical to modern precision measurement. Currently, LIGO utilizes a 1064 nm laser in a Fabry-Perot Michelson interferometer to measure the perturbations to lengths resulting from a passing gravitational wave[1][2]. However, the exceedingly small amplitude of these perturbations requires exceedingly careful attention to sources of noise in the detectors, even after scaling the interferometer up to 4 km. A substantial component of LIGO's current noise budget is the thermal noise of the fused silica 'test masses' (mirrors)[2]. To reduce the contribution of thermal noise in the detector, a shift to cryogenic optics after the O5 observing run has been proposed in the LIGO Voyager upgrade to the LIGO Hanford and Livingston Observatories[3]. Additionally, KAGRA and proposed 3rd Generation Observatories such as the Einstein Telescope and advanced models of LIGO Cosmic Explorer incorporate cryogenic optics for the reduction in thermal noise[2]. Unfortunately, the transition to cryogenic optics requires modifications to several existing design choices. The fused silica currently used as the test mass substrate is incompatible with the cryogenic system, requiring a transition to another substrate. KAGRA uses saphire as its substrate, but the favored substrate is crystalline silicon. Crystalline silicon has favorable thermal characteristics, but is unusably absorbant to light at 1 µm, requiring a transition to 1.5 µm-2 µm lasers[2]. For Voyager, the primary contender is 2050 nm[4].

The 2 µm laser is additionally of interest to LIDAR and carbon dioxide measurements for its transparency in air and absorption by carbon dioxide[5][6]. However, the state of technology at the 2 µm wavelength is notably behind that which has been developed at 1064 nm[2]. Particularly for the precision of interferometric measurements, the lasers must have narrow linewidths (range of light frequencies output) to reduce noise coming from other wavelengths. Current 2050nm lasers reach linewidths around 50kHz at low power, with more powerful lasers demonstrating much broader linewidths[4]. To achieve narrower linewidths suitable for more precise measurements, the laser phase noise must be reduced using a control circuit. A common method involves selecting out the primary frequency using a resonant cavity and returning a control feedback loop to the laser source to lock the laser to the resonant mode of the cavity. Under the right circumstances, this can achieve linewidths less than a millihertz in the optical range, yet requires costly precision optics and cannot operate at high frequencies

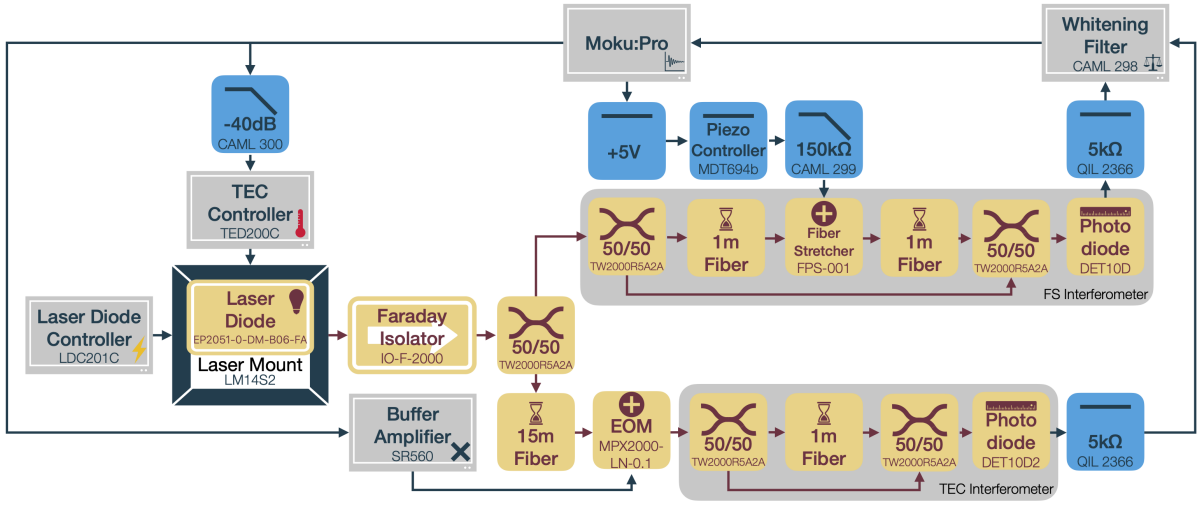

Figure 1: Diagram of the Optical Setup

where the control delay exceeds the correlation time of the noise[7]. In the 2018 LIGO SURF Program, Vinicius Wagner demonstrated this approach to phase noise reduction at 2 µm[8].

This experiment serves to investigate an alternate method of phase noise reduction, feedforward. In this mode, the phase noise is measured in real-time on a sample of the beam using an interferometer, and a correction term is calculated while the bulk laser is propagating through a delay line. Then, the adjustment is applied to the bulk laser following the delay line to correct for the measured phase noise. This approach has the benefit of being able to directly respond to the deviations in phase, while having the drawback of a more open control system, making the system more vulnerable to drifts in component gain. The direct response decreases the latency from measurement to actuation with respect to the signal, allowing for performance at frequencies outside the capacity of typical feedback systems, into the MHz range.

3 Approach

This work draws substantively from previous work in feedforward linewidth stabilization[9][10]. As detailed in Fig. 1, the beam from a 2 µm laser (e.g. [11]), following a Faraday isolator for the protection of the diode, is split in two via a 50:50 beam coupler, with half of the beam being sent into a fiber-optic delay line of approximately 15 m (approximately 75 ns delay). While the light propagates through the delay line, the other portion of the beam is sent into a homodyne Mach-Zehnder interferometer to measure its phase error.

The interferometer consists of a 50:50 coupler to split the beam in half, a short delay line for one half, and interfering the delayed half with the direct beam in a second 50:50 coupler. To maintain the interferometer response in the linear regime around 90° phase difference between legs so that the response has maximum predictable gain, a control element must compensate for frequency drifting. A piezoelectric fiber stretcher in the delay line is used for the stabilization of the FS interferometer, and feedback to the temperature of the laser diode is used to stabilize the other, TEC interferometer. This control is limited to the sub-10 Hz

frequency band, with higher-frequency variations being unsuppressed. The light output of the hybrid is then converted into electrical signals using a photo-detector, and decomposed into component frequencies by the Moku Spectrum Analyzer, normalized by the bandwidth of each frequency bin. This yields an amplitude spectral density, or the root mean square noise power spectrum. Via a measurement of the amplitude of the fringe over a full 2π sweep, this is converted from volts to radians, as $V_{out} = V_0 + V_1 \cos\Delta\phi$, or in the linear regime $V_{out} = V_0 + V_1(\Delta\phi - \frac{\pi}{2})$. This equates to a measurement of the correlation of the phase deviations between the direct and delayed beams, allowing for a measurement of the frequency noise, related by $\phi(t) = 2\pi f(t)/\tau$, with τ representing the relative delay between the two arms.

This approach also requires a few supporting electronic components to adapt the signals between devices. A whitening filter between the photodetectors and the ADC suppresses the contribution of the ADC noise to the measurement by increasing the magnitude of low-amplitude high-frequency components without amplifying the DC component that would otherwise saturate the ADC. Additional filters were created to shift the Moku output $[-5\,\mathrm{V}, 5\,\mathrm{V}]$ to $[0\,\mathrm{V}, 10\,\mathrm{V}]$, attenuate the input signal to the TEC by 40 dB for more precise control, and suppress high-frequency noise from being injected into the system by control elements. This setup also allows for a pair of balanced photodetectors which would allow for an increased rejection of intensity noise in the phase noise measurement if the intensity noise becomes a limiting error source in the accurate phase noise measurement.

Digital circuitry in the Moku then applies an appropriate gain to this measured phase noise in the FS Interferometer before outputting a phase correction RF signal to control an electro-optic modulator at the end of the primary branch's delay line, prior to entering the TEC interferometer. Following the application of this correcting frequency shift, the resultant laser output is expected to contain reduced phase noise, measured via the TEC Interferometer.

4 System Model

So that the system can be properly understood and the performance limits estimated, the system's transfer functions and noise sources have been modeled, resulting in the production of a noise budget for the system, Fig. 2. This involves first measuring and/or theoretically modeling transfer functions between points in the system.

To minimize the number of measurements contributing to the calculations, the laser power in each interferometer is measured directly prior to the 50:50 coupler. Then, to first order, the power output of the interferometer is half the sum of the two inputs. Power fluctuations of the laser transfer to the output directly as half their value prior to the 50:50 coupler. Frequency fluctuations in the laser transfer to power output as $V_1(2\pi\Delta f/\tau)$ with V_1 as the amplitude of the fringe, and τ as the time delay between the arms.

The power output from the interferometer is then transferred to electrical signals by the sensitivity of the photodiode with the transimpedance amplifier. The DC gain was measured by the varying output in response to differing laser power inputs. This was verified to correspond to the AC gain through the frequency band the response to an AC oscillation in the laser power and a measurement of the shot noise when it dominates at high frequency.

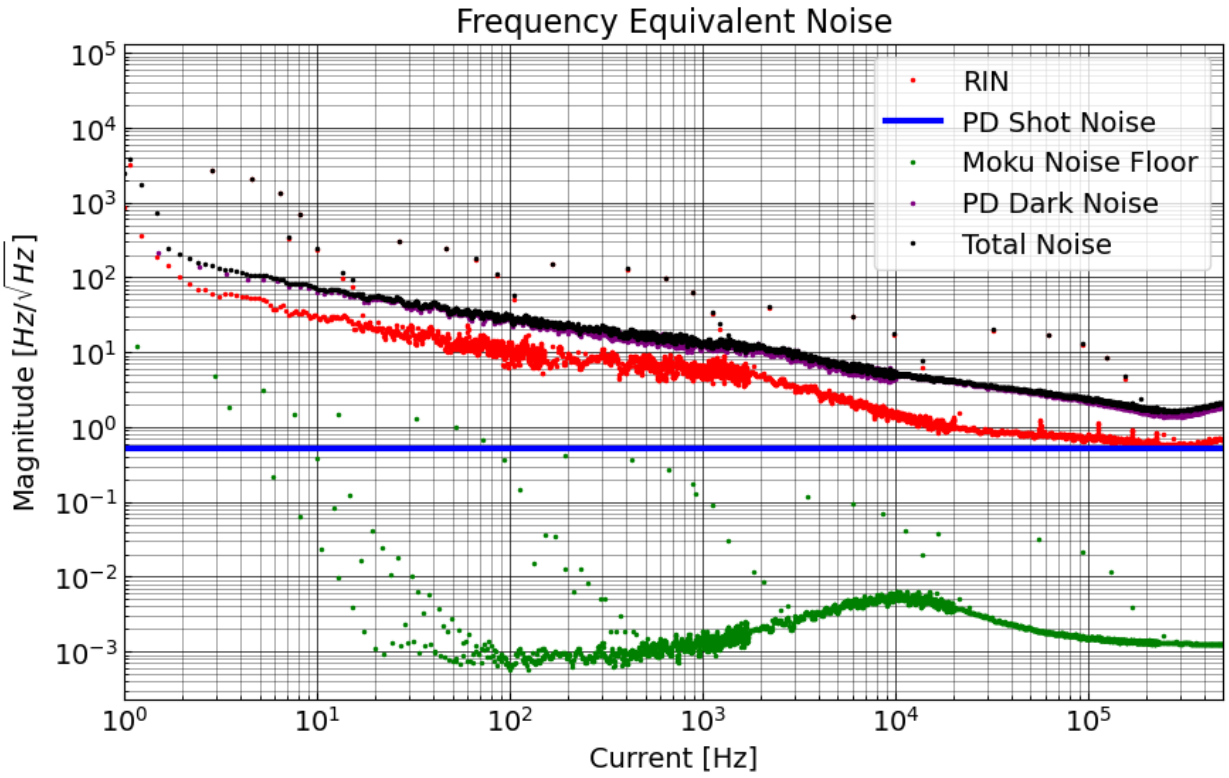

Figure 2: Noise Budget of First Interferometer

Then the whitening filter adds to the model transfering the initial electrical signals to a whitened signal. This transfer function was measured via a swept sine measurement on a SR785 Dynamic Signal Analyzer. Through a combination of these functions, signals can be converted from their source to equivalent frequency noise or noise at the Moku input.

The noise sources modeled include the photodiode shot noise, the relative intensity noise of the laser, the Moku noise floor, and the photodiode dark noise. The relative intensity noise of the laser is measured as the AC component from the laser landing directly on the photodiode in frequency space and then dividing out the DC laser power. Its contribution to the interferometer setup to first order is then the RIN multiplied by the DC power on the photodiode. The shot noise at the photodiode is calculated from the average power on the photodiode as $\sqrt{2P\hbar c/\lambda}$, or equivalently the electrical as $\sqrt{2eI}$. Photodiode dark noise is measured as the signal from the photodiode with the laser off, and Moku Input noise is measured as the signal from the Moku with the inputs terminated.

Then, measurements of the amplitudes of the noise sources across the frequency domain are moved through the system via these transfer functions to produce their equivalent frequency noise and summed in quadrature to calculate the total noise of the system. This model can then used to predict the limiting factors for the measurement of the initial and final noise and the expected amount of noise reduction.

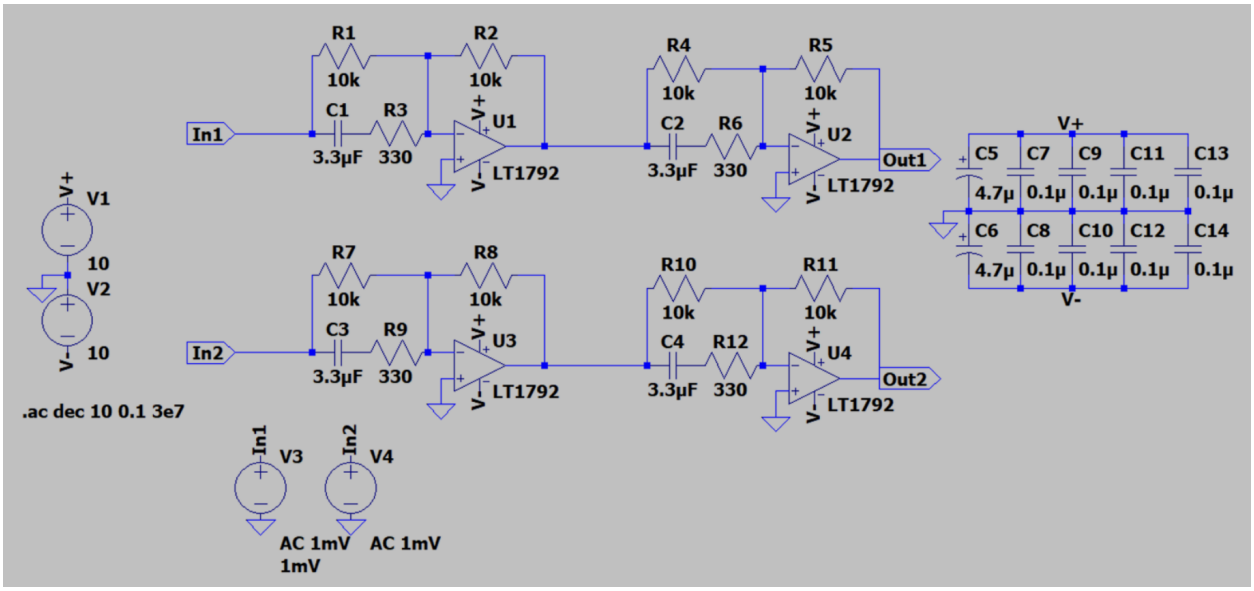

Figure 3: Circuit Diagram for the Whitening Filter

5 Circuitry

The circuit for the whitening filter was inspired by the topology used in [12] and adapted to fit the gains and frequency ranges used in this project along with using non-differential inputs/outputs, resulting in the circuit topology shown in Fig. 3. This circuit increases the magnitude of the AC components between 100 Hz and 300 kHz by a factor of 1000 so that they can clearly be measured above the noise floor of the Moku while also allowing for the measurement of the larger DC component for locking the interferometer. Additional circuits were made for the conditioning of other signals, including the −40 dB filter which uses a passive resistive divider to decrease the magnitude of the signal by a factor of 100, and a capacitor to low-pass the signal, rejecting high-frequency noise above 4 Hz. The 150 kΩ circuit increases the output impedance of the piezo-controller so that the capacitance of the fiber-stretcher rejects high-frequency noise from the piezo-controller while the 5 V circuit uses a summing amplifier to shift the output of the Moku by 5 V so that it spans the input range of the piezo-controller. The 5 kΩ circuits are transimpedance amplifiers built by Dr. Koji Arai at the lab for a prior experiment to convert the current output of the photodiodes to voltages for measurement.

6 Reduction Result

After constructing the system, we locked both interferometers using integral gain in the Moku, using the PID instrument in multi-instrument mode. Then, using the Moku digital filter box to construct the feedforward signal and the Moku spectrum analyzer to measure the noise, we observed a preliminary reduction in phase noise, Fig. 4. This result had the issue of increasing the noise in adjacent frequency ranges and only reducing the noise in a narrow range. Additionally, this cancellation was not stable over time, with the reduced band moving through the range. This variance likely derives in part from the varying phase

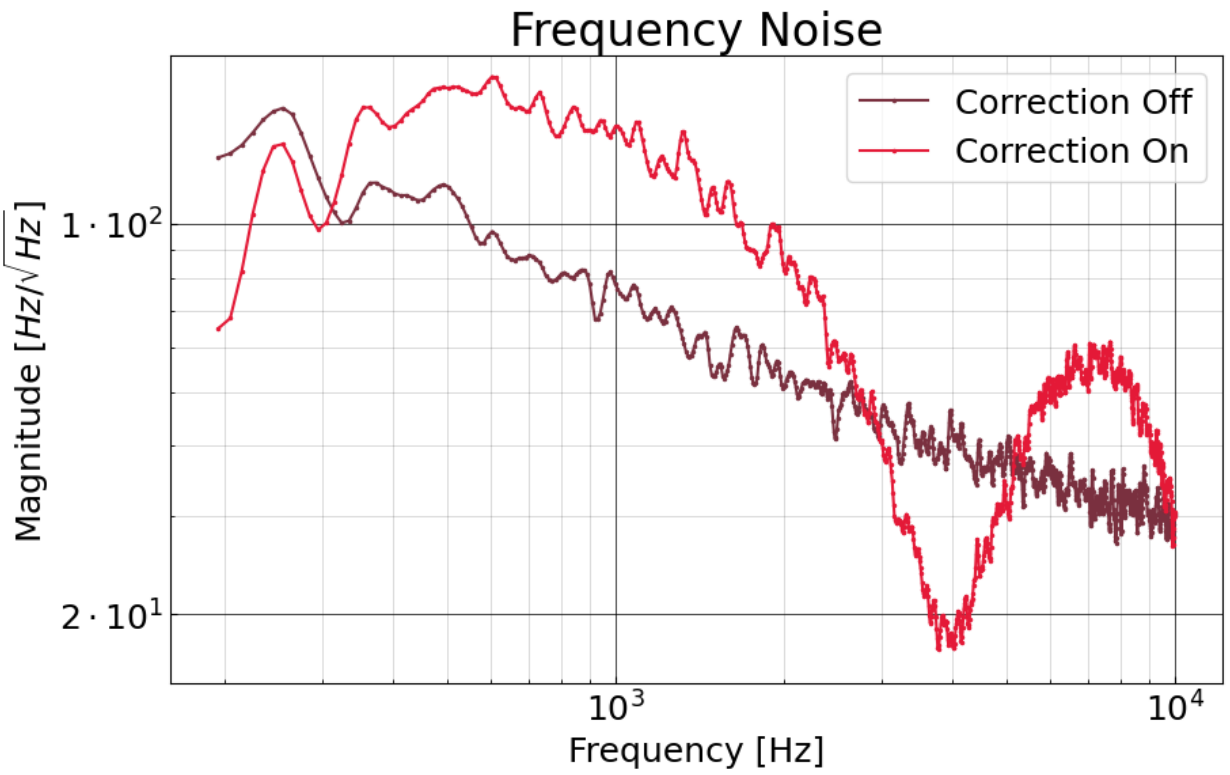

Figure 4: Decreased Phase Noise

throughout the frequency band in the gain used for the feedforward, as seen in Fig. 5. This can likely be compensated by using a broader frequency band for the feedforward gain. Additionally, the optical delay is only about 50 ns while the electrical delay is closer to 500 ns. This mismatch limits the ability for the system to suppress noise at higher frequencies, as this noise is not coherent between the measurement and actuation.

7 Continuing Work

The next steps for this project include producing a prediction for maximum noise cancellation given the noises in the system and achieving this noise cancellation on a more substantive range of frequencies. This involves completing the analysis of the system and its actuators, attempts to reduce the electrical delay by shortening cables, using an alternate digital or analog control box, increase the length of the optical delay, and work to thermally insulate the system to increase stability in the delays. It may also be beneficial to have a procedure to more precisely set the feedforward gain and perhaps have it dynamically update to ensure proper matching between the actuation and noise. This system can also be tested on other lasers which begin with less frequency noise and used in conjunction with established laser feedback methods, so that the resulting beam would be more suitable for gravitational wave interferometry.

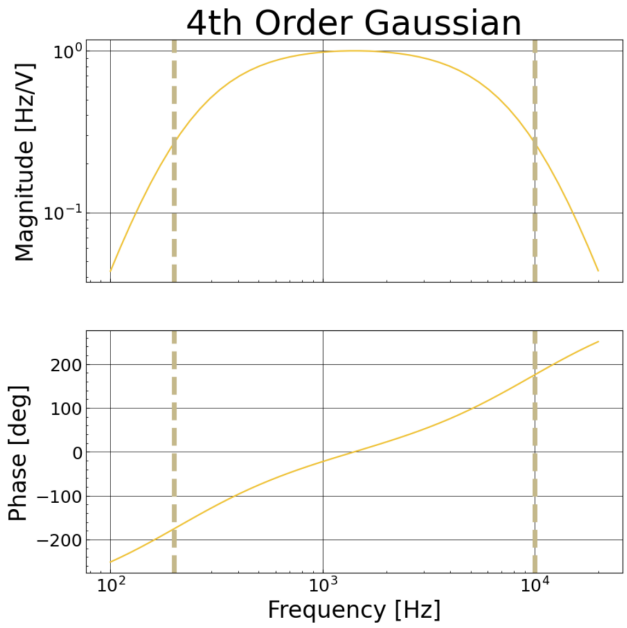

Figure 5: Feedforward Gain

8 Acknowledgements

Thank you to the Caltech Class of '52 Named SURF Fellowship and the National Science Foundation for supporting my summer research. Additional thanks to LIGO Lab and Caltech for hosting the project, my mentors Professor Rana Adhikari and Dr. Aidan Brooks, and my collaborator Stella Krauss.

References

[1] S. Ballmer, V. Mandic, L. Barsotti, C. Berry, S. Bose, D. Keitel, Z. Marka, D. Ottaway, J. Read, S. Reid, J. Romano, J. Romie, J. Sanders, P. J. Sutton, D. Reitze, A. Lazzarini, and P. Brady, "Ligo scientific collaboration program (2022 edition)." Online, Sept. 2022. LIGO DCC M2200183-v2.

[2] P. Fritschel, F. Schiettekatte, G. Vajente, L. McCuller, D. Brown, V. Quetschke, J. Steinlechner, and B. Slagmolen, "The LSC instrument science white paper (2022-2023 edition)." Online, May 2023. LIGO DCC T2200384-v2.

[3] V. Mitrofanov, "Ligo voyager project of future gravitational wave detector." Online, Nov. 2016. LIGO DCC G1602258-v2.

[4] R. Adhikari, A. Brooks, K. Araj, and C. Wipf, "Voyager Meeting 16-Nov-2021: Wavelength Choice." Online, Nov. 2021. LIGO DCC L2100089-v1.

[5] S. H. Hosseini, "Study of 2 Micron Laser," in *University of Arizona Masters Theses*, The University of Arizona., 2022. Journal Abbreviation: University of Arizona Masters Theses.

[6] J. Yu, M. Petros, Y. Bai, S. Chen, J. Lu, and U. Singh, "A Pulsed 2-micron Coherent Differential Absorption Lidar for Atmospheric CO2 Measurements," in *Lasers, Sources, and Related Photonic Devices*, p. LT5B.1, Optica Publishing Group, 2012. Journal Abbreviation: Lasers, Sources, and Related Photonic Devices.

[7] T. R. Schibli, I. Hartl, D. C. Yost, M. J. Martin, A. Marcinkevičius, M. E. Fermann, and J. Ye, "Optical frequency comb with submillihertz linewidth and more than 10 W average power," *Nature Photonics*, vol. 2, no. 6, pp. 355–359, 2008. ISBN: 1749-4893.

[8] V. Wagner, A. Wade, A. Brooks, and R. Adhikari, "Stabilization of a 2 µm laser using an all-fiber delay line mach-zehnder interferometer." Online, Nov. 2018. LIGO DCC T1800238-v1.

[9] J. Chen, Q. Liu, and Z. He, "Feedforward Laser Linewidth Narrowing Scheme Using Acousto-Optic Frequency Shifter and Direct Digital Synthesizer," *Journal of Lightwave Technology*, vol. 37, no. 18, pp. 4657–4664, 2019.

[10] H. Tian, F. Meng, K. Wang, B. Lin, S. Cao, Z. Fang, Y. Song, and M. Hu, "Optical frequency comb stabilized to a fiber delay line," *Applied Physics Letters*, vol. 119, no. 12, p. 121106, 2021. _eprint: https://doi.org/10.1063/5.0062785.

[11] Eblana Photonics, Dublin, Ireland, *2004nm DM LASER EP2004-DM-B*, 2015. Available at https://eblanaphotonics.com/wp-content/uploads/2020/11/EP2004-DM-B.pdf, Rev 2.1.

[12] S. J. Miller, J. Lough, and N. Mukund, "Improved whitening of the readout signal for geo 600," *UFlorida IREU*, 2019.